

# Facile Synthesis of Copper Iodide at Low Temperature as Hole Transporting Layer for Perovskite Solar Cell

Omsri Vinasha Aliyasevram\*<sup>id</sup>, Faiz Arith\*<sup>‡</sup><sup>id</sup>, Ing Jia Rong\*<sup>id</sup>, Shahril Izuan Zin\*<sup>id</sup>, Fara Ashikin Ali<sup>id</sup>\*\* and Ahmad Nizamuddin Mustafa\*\*\*<sup>id</sup>

\*Faculty of Electronic and Computer Engineering, Universiti Teknikal Malaysia Melaka, Hang Tuah Jaya, 76100 Durian Tunggal, Melaka, Malaysia

\*\*Faculty of Electrical and Electronic Engineering Technology, Universiti Teknikal Malaysia Melaka, Hang Tuah Jaya, 76100 Durian Tunggal, Melaka, Malaysia

\*\*\*Material Department, Faculty of Engineering, Imperial College London, London SW7 2AZ, United Kingdom  
m022020014@student.utem.edu.my; faiz.arith@utem.edu.my; jiaronging@gmail.com; shahril@utem.edu.my; fara@utem.edu.my; nizamuddin@utem.edu.my

<sup>‡</sup>Corresponding Author; Faiz Arith, Faculty of Electronic and Computer Engineering, Universiti Teknikal Malaysia Melaka, Hang Tuah Jaya, 76100 Durian Tunggal, Melaka, Malaysia

E-mail: faiz.arith@utem.edu.my

*Received: 23.02.2022 Accepted: 30.03.2022*

**Abstract-** A highly conductive Copper Iodide, (CuI) as solid-state hole transporting layer (HTL) with homogenous particles are produced by a two-step spin-coating method at room temperature with controlled conditions along with an optimized thermal annealing process at low-temperature condition. Conventional CuI films demand high annealing temperature for the fabrication process resulting in unsuitable for flexible applications. Primarily, thermal annealing has a major impact on the structural and electrical properties of the CuI thin films. Thus, to study the influence of thermal annealing, the fabricated CuI films were characterized for their surface morphology and crystallinity by utilizing Scanning Electron Microscope (SEM), X-Ray Diffraction (XRD) and Raman Spectroscopy, respectively. Moreover, electrical characterization revealed the conductivity of the fabricated CuI films. The thermal annealing temperature of CuI HTL was optimized to 100 °C, yielding an immaculate morphological structure and a high electrical conductivity of 57.75 S/m.

**Keywords** CuI, Hole Transporting Layer, Perovskite Solar Cell, Spin-Coating.

## 1. Introduction

Currently, the conventional silicon-based solar cell is suffering from the high fabrication costs that involved sophisticated and vacuum-based equipment [1–3], whereas Perovskite Solar Cells (PSCs) have evolved rapidly, a two-fold increase in cell efficiency in less than two decades [4–7], offering a wide absorption spectrum [8] and strong Power Conversion Efficiency (PCE) at minimal manufacturing costs [9]. Yet, the employment of liquid-based electrolytes as Hole Transport Layer (HTL) in emerging solar cell technologies has a decisive disadvantage as it disrupts device

stability due to heat-induced liquid evaporation, contamination, and leakage as the reaction between oxygen molecules or water molecules with the electrolyte occurs inside the cell [10], [11]. Hence, solid-state HTL material is the potential alternate for liquid-based electrolytes in PSCs construction to uphold its robustness and efficiency over a long period [12, 13].

Lately, the copper-based materials as inorganic HTL have presented convincing performance of PSCs [14], to replace the unstable organic material HTL, namely spiro-OMeTAD [15] and PEDOT: PSS [16]. However, solution-

processed Copper Thiocyanate (CuSCN) exhibits exceptionally high series resistance on the fabricated films leading to low electrical performances [17, 18]. Ideally,

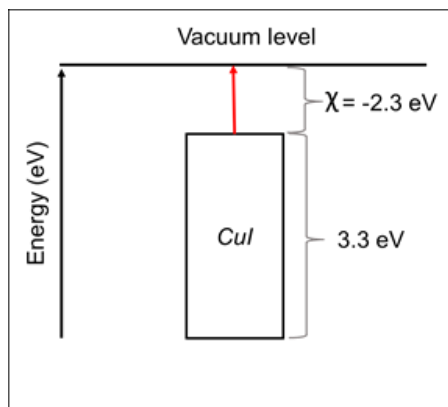


**Fig. 1.** Schematic band diagram of CuI with 3.1 eV.

Cuprous Iodide, (CuI) shows decent hole conductivity with solid p-type semiconductor properties and a broad bandgap of  $\sim 3.1 \text{ eV}$  deploy as HTL via a facile synthesis method under optimization [19, 20] as depicted in Figure 1 below. CuI is a unique water-insoluble material that exhibits p-type nature due to copper vacancies in the lattice and proved that the doping technique stabilizes the crystal lattice with divalent and trivalent cations as required for the charge compensation [21, 22].

After years of comprehensive experiments, Tennakone *et al.* documented the significant role of CuI as hole collecting and transporting material in new emerging solar applications [23–26]. CuI is discovered as an alternative for organic HTLs towards highly efficient photovoltaic [22, 27] and optoelectronic devices [28] by proving a high transmittance of 60–85% in the visible spectrum range [29] and achieving high room-temperature conductivity despite the degeneration [30, 42].

Recently, various methods are experimented with for CuI film preparation, such as using spin coating [32], mist-atomization [33, 34], thermal evaporation [35, 36], Focused Ion Beam (FIB) [31], chemical deposition [37, 38] and reactive sputtering [30, 39]. Li *et al.* Apparently, numerous experiments contended that there are several factors such as the thickness of layer [40], growth temperature, copper vacancies [41], numbers of coating cycles, use of solvent and additives, are highly influencing the physical and electronic properties of CuI [42, 43].

Thermal annealing of copper-based material has a pivotal role in its electronic properties as it alters the physical and chemical characteristics of the material [44, 45]. In this context, Kaushik *et al.* [46] proved that annealing is vital to solar cell efficiency as the growth temperature impacts the resistivity, thereby affecting the charge carrier density and conduction of the CuI thin films prepared of the deposited layers. Yet, T. Prakash [45] documented that annealing of CuI samples beyond  $300 \text{ }^\circ\text{C}$  induces copper melting, and iodine loss based on his SEM images and TG-DTA results, respectively. Indeed, Mulla *et al.* [47] theorized that annealing of CuI at inefficacious conditions causes changes

in defect chemistry and charge distribution which alters electrical properties as their research outcome denoted a reduction of iodine content after annealing. Therefore, optimization of temperature for thermal annealing is essential for achieving high photovoltaic efficiency as it strengthens the charge carrier mobility of Cu [48].

The present work aims to propose a simple solution-processed method of CuI as HTL and to study the impact of thermal annealing on structural and electrical properties of the fabricated CuI films. Furthermore, when creating the precursor solution for deposition on ITO coated glass substrate, the thermal annealing condition is optimized at a low-temperature condition without the need for additional solvent additives.

## 2. Methodology

### 2.1. Deposition of CuI

ITO coated glass substrates were inserted in a beaker filled with ethanol and positioned in an ultrasonic cleaner. The ultrasonic cleaners employ ultrasonic sound to alternately radiate the liquid in the bath with high and low pressure to remove undesirable contaminations from the substrate. The ultrasonic cleaner was set to run for 10 min, and after 10 min, the glasses were placed on a digital hot plate at  $70 \text{ }^\circ\text{C}$  for 20 min.

As to prepare CuI precursor solution, 120 mg of CuI powder was weighted. Then, 6 ml of ethylene glycol was mixed with CuI powder in a beaker. Then, the procedure has proceeded with 50 min of solution dilution using an ultrasonic bath at  $70 \text{ }^\circ\text{C}$ . Before starting with an ultrasonic bath, the beaker was covered with aluminium foil.

The CuI layer was deposited on ITO coated glass substrate by spin-coater as CuI solution dripped ten times for each sample. Then spin-coater was set to spin twice, which are 500 rpm for 5 s and 2500 rpm for 30 s. The first spin-coating formed a smooth uniform surface, whereas the second spin-coating created a thin layer on the ITO coated glass substrate. Lastly, thermal annealing process was performed on a digital hot plate for 10 min, at various temperatures for each CuI sample, such as  $70 \text{ }^\circ\text{C}$ ,  $80 \text{ }^\circ\text{C}$ ,  $100 \text{ }^\circ\text{C}$ ,  $150 \text{ }^\circ\text{C}$ , and  $200 \text{ }^\circ\text{C}$ .

### 2.1. Deposition Characterization

Scanning electron microscopy (SEM) measurements were performed utilizing the EVO 18 from ZEISS Research Microscopy Solutions at different magnifications with a 15 kV of operating voltage and a 5.5 mm of working distance, to detect a cross-sectional and planar view image of the material surface as well as the particle growth density. Furthermore, the PANalytical X'Pert Pro X-ray diffraction (XRD) was used to identify crystal structure and surface morphology features of the deposited layers, by performing powder diffraction at an incident angle of  $10^\circ$  with Ceramic Cu K $\alpha$  radiation of 1.5406 Å. Likewise, UniRAM-3500, Raman spectroscopy was employed used to obtain the

Raman shift graph of the deposited CuI layer, determining the chemical composition of the material by detecting vibrational, rotational, and other states in a molecular system. Besides, I-V characterization which demonstrates the electrical properties of CuI thin films were analyzed using Keithley model-2400, a digital source meter in two-probe analysis mode with a sweep step size of 40 mV.

### 3. Results and Discussion

#### 3.1. Structural performance of CuI

The SEM images of CuI annealed at different temperatures are recorded in Figure 2. The images are enlarged up to 10000 times to ascertain the physical structure of CuI annealed on ITO coated glass substrate. The structure of CuI particles in both Figure 1 (a) and (b), are not fully crystallized and less dense for the annealing temperature at 70 °C and 80 °C, respectively. As depicted in Figure 2 (c) and Figure 3, the CuI particles clearly shows high density and uniformity in grain growth when annealed at 100 °C. Additionally, SEM images in Figure 2 under various magnification like 20, 500, 2000, 5000 and 7000 times revealed that CuI annealed at 100 °C has produced crystal-shaped CuI particles over a large area.

However, the structure of CuI particles is dense, yet start to melt away from the physical structure as shown in Figure 2 (d) which annealing temperature at 150 °C. Likewise, the CuI particles in Figure 2 (e) that are annealed at 200 °C display melting behaviour, as the structure is obviously changed to other forms and might be due to overheating [49]. In this context, the crystallization happens quickly, thus difficult to regulate as creates a chain-like structure with a gap between them. Here, insufficient dispersion of the crystals might be affected by the thermal condition, particularly the annealing process during the fabrication of the material [50].

Besides, temperature condition higher than 100 °C deteriorates the cell's structural properties due to variations in the charge carrier mobility of CuI. Although CuI particles move rapidly in all directions, they tend to bump into other particles more frequently in a solid-state phase than in a liquid phase due to brisker spaces between the arrangement of particles [31]. Conclusively, optimization of thermal annealing is crucial for fabricating high performing films, thereby thermal annealing temperature at 100 °C is the most appropriate for CuI HTL based on the SEM results and further electrical characterization is analyzed to confirm.

In addition, the CuI film's crystalline structure is determined by using an XRD pattern. Figure 4 elucidates the corresponding peaks on the graph of intensity versus  $2\theta$  of CuI and ITO based on the resulting XRD data. The CuI diffraction peaks at 21.3°, 25.5°, 37.4°, and 45.3° correlate to the (111), (111), (210), and (220) planes of CuI, respectively. Correspondingly, there are a few peaks that belong to ITO according to JCPDS Card No. 00-001-0929 with the main peak position at 30.8°.

The Raman spectrum is acquired by performing Raman spectroscopy which examines the inelastic light scattering by

the vibrational response of the material. The crystallinity of the material is analyzed by the change in molecular energy caused by inbound photons interacting with bond vibrations that indicates the material structure [51]. The Raman spectrum in Figure 5 depicts the scattered light intensity as a feature of the Raman shift expressed as a wavenumber, hence

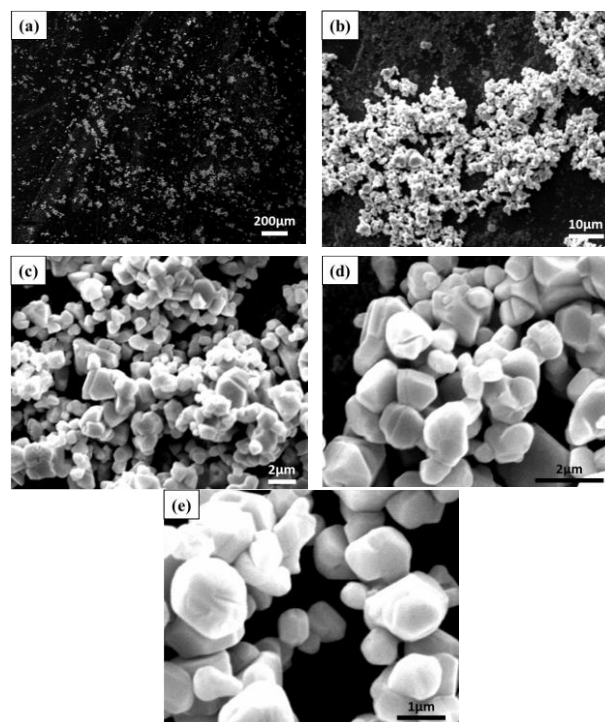


**Fig. 2.** SEM images of the surface morphology of the fabricated CuI layers and thermally annealed at various temperatures.; (a) 70 °C, (b) 80 °C, (c) 100 °C, (d) 150 °C, and (e) 200 °C.

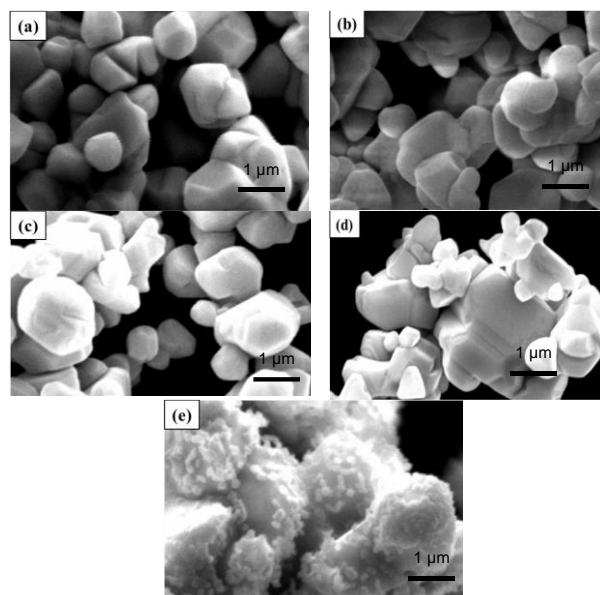


**Fig. 3.** SEM images of the surface morphology of the fabricated CuI layers and thermally annealed at 100 °C under various magnifications; (a) 20, (b) 500, (c) 2000, (d) 5000, and (e) 7000.

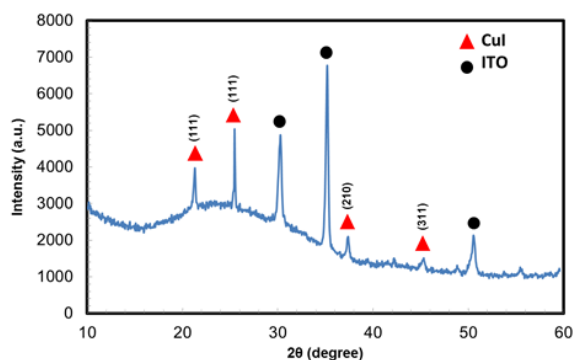


**Fig.4.** XRD analytical result of CuI film deposited on ITO coated glass substrate.

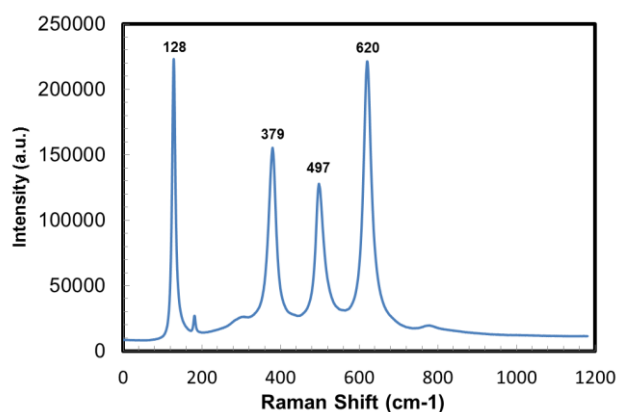


**Fig. 5.** Raman spectrum of CuI HTL deposited on ITO coated glass substrate.

simply proving that the deposited thin films are made up of CuI elements. As well, Raman peaks of the CuI substrate are at  $128\text{ cm}^{-1}$ ,  $379\text{ cm}^{-1}$ ,  $497\text{ cm}^{-1}$  and  $620\text{ cm}^{-1}$ . The ultimate Raman peak is recorded at  $128\text{ cm}^{-1}$  which showed an intensity of 223 212, while the peak of  $128\text{ cm}^{-1}$  indicated the presence of CuI on top of the ITO coated glass substrate. The intensity of the other peaks such as 155 425, 127 927, and 221 438 correspond to the Raman shift of  $379\text{ cm}^{-1}$ ,  $497\text{ cm}^{-1}$ , and  $620\text{ cm}^{-1}$ , respectively.

### 3.2. Electrical performance of CuI

I-V characteristics are evaluated by 2-probe mode analysis via Keithley 2400 with a voltage supply ranging from 0.5 V to 4 V, to evaluate the current of ITO and CuI samples five times. With that, mean, standard deviation and error bar of measured current were computed to observe the linear current-voltage curve corresponding to Ohm's law. In that case, I-V characteristics as exemplified in Figure 5 validate that the measured current is directly proportional to the applied voltage.

As per Figure 6, the gradient of ITO glass is 51.31 acts as the baseline for the fabricated CuI samples. Essentially, the gradient of CuI higher than ITO coated glass indicates the better electrical conductivity of CuI. The CuI

substrates annealed at  $100\text{ }^\circ\text{C}$  exhibited the electrical conductivity higher than ITO coated glass which is 57.75 S/m. By comparison, CuI annealed at  $70\text{ }^\circ\text{C}$ ,  $80\text{ }^\circ\text{C}$ ,  $150\text{ }^\circ\text{C}$  and  $200\text{ }^\circ\text{C}$  displayed lower electrical conductivity of 45.56 S/m, 46.56 S/m, 47.90 S/m and 45.44 S/m respectively, thereby inferring to low electrical performance than ITO coated glass as charted in Figure 7. Likewise, Murmu *et al.* [52] reported a comparable result of CuI films with an electrical conductivity of 22.9 S/m.

Despite applied voltages impacting the electrical conductivity of the material, the grain size of nanocrystalline materials commonly has an explicit influence on the electronic current flow [14]. The electrical conductivity of the CuI film is mostly determined by the size of the CuI particles, which affects the hole mobility of CuI atoms [53], [54]. The SEM images of Figure 1 (d), distinctly shows that CuI film annealed at  $100\text{ }^\circ\text{C}$  produced smaller sized grains in the nanometer regime, thus revealing in highest conductivity as nanometer-sized crystallites are extremely sensitive to absorb and harvest the light [55].

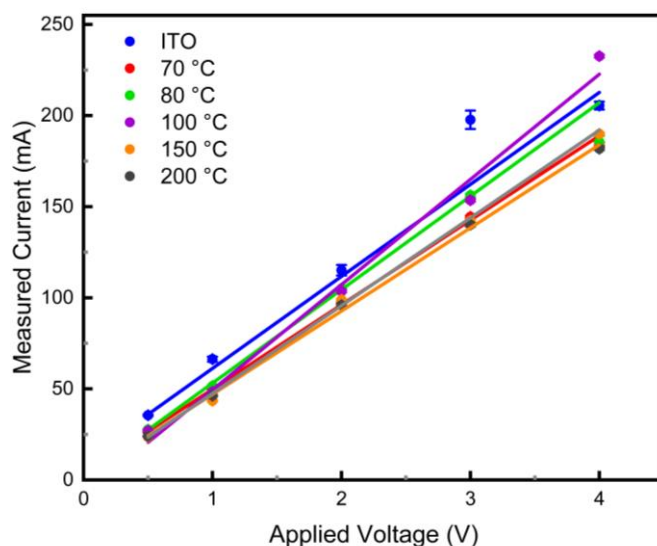


**Fig. 6.** I-V characteristics of CuI at different temperatures,  $70\text{ }^\circ\text{C}$ ,  $80\text{ }^\circ\text{C}$ ,  $150\text{ }^\circ\text{C}$ ,  $200\text{ }^\circ\text{C}$ .

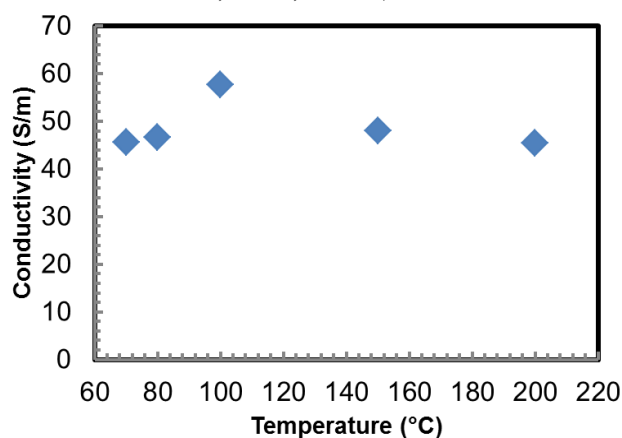


**Fig.7.** The conductivity of all CuI thin films at the different annealing temperatures of  $70\text{ }^\circ\text{C}$ ,  $80\text{ }^\circ\text{C}$ ,  $150\text{ }^\circ\text{C}$  and  $200\text{ }^\circ\text{C}$ .

Meanwhile, the CuI film annealed at  $150\text{ }^\circ\text{C}$  with larger grains as shown in Figure 2 (e), offers lower conductivity.

Here, phonon scattering is commonly related to thermal conductivity [56], as the wide grain boundaries may have caused phonon scattering and altered the electron and hole mobility of CuI atoms [57]. Henceforth, the best electrical conductivity obtained from the I-V curve is the CuI layer annealed at 100 °C as well as recommended to anneal at 100 °C since it comparatively delivers the most excellent electrical performance than other samples.

#### 4. Conclusion

HTL of PSCs can alter the efficacy of PCE as it plays a crucial role because it inhibits electron transmission to the back-contact metal electrode, extracts photo-generated holes from the perovskite, and transports these extracted charges back to the back-contact metal electrode. CuI is introduced as inorganic HTLs to substitute the conventional liquid-based electrolytes, by depositing on top of ITO coated glass substrate via a spin-coater. The spinning speed and time are controlled for the two-step spin-coating technique. Besides, the thermal annealing temperature of CuI films is optimized based on the structural and electrical performance, determined by Scanning Electron Microscopy (SEM), X-Ray Diffraction (XRD) and Raman Spectroscopy, and I-V characterization, respectively. Although applied voltages affect the material's electrical conductivity, the grain size of nanocrystalline materials has a substantial effect on electrical current flow. SEM images of CuI films at 100 °C showed uniformity in particle size and crystalline compared with other annealing temperatures with the highest conductivity of 57.75 S/m. Therefore, CuI films that are thermally annealed at 100 °C are suggested to offer high stability to the PSC structure.

#### Acknowledgements

The research of O. V. Aliyaselvam was financed by the Zamalah Scheme, Universiti Teknikal Malaysia Melaka, Malaysia.

#### References

- [1] S. Sharma, K. K. Jain, and A. Sharma, "Solar Cells: In Research and Applications—A Review," *Materials Sciences and Applications*, vol. 06, no. 12, pp. 1145–1155, 2015.
- [2] K. Ranabhat, L. Patrikeev, A. A. evna Revina, K. Andrianov, V. Lapshinsky, and E. Sofronova, "An introduction to solar cell technology," *Journal of Applied Engineering Science*, vol. 14, no. 4, pp. 481–491, 2016.
- [3] M. A. Green, "Third generation photovoltaics: Solar cells for 2020 and beyond," *Physica E: Low-Dimensional Systems and Nanostructures*, vol. 14, no. 1–2, pp. 65–70, 2002.
- [4] H. S. Jung and N. G. Park, "Perovskite solar cells: From materials to devices," *Small*, vol. 11, no. 1, pp. 10–25, 2015.
- [5] H. Sun, S. Lin, R. Zhang, K. Yang, M. Xia, W. Li, and W. Guo "Perovskite solar cells employing Al<sub>2</sub>O<sub>3</sub> scaffold layers," *2014 International Conference on Renewable Energy Research and Application (ICRERA)*, Milwaukee, pp. 442–444, October 2014.
- [6] M. Grätzel, "Dye-sensitized solar cells," *Journal of Photochemistry and Photobiology C: Photochemistry Reviews*, vol. 4, no. 2, pp. 145–153, 2003.
- [7] M. Green, E. Dunlop, J. Hohl-Ebinger, M. Yoshita, N. Kopidakis, and X. Hao, "Solar cell efficiency tables (version 57)," *Progress in photovoltaics: research and applications*, vol. 29, no. 1, pp. 3–15, 2021.
- [8] A. Kojima, K. Teshima, Y. Shirai, and T. Miyasaka, "Organometal halide perovskites as visible-light sensitizers for photovoltaic cells," *Journal of the American Chemical Society*, vol. 131, no. 17, pp. 6050–6051, 2009.
- [9] M. A. Green, A. Ho-Baillie, and H. J. Snaith, "The emergence of perovskite solar cells," *Nature Photonics*, vol. 8, no. 7, pp. 506–514, 2014.
- [10] N. H. Tiep, Z. Ku, and H. J. Fan, "Recent Advances in Improving the Stability of Perovskite Solar Cells," *Advanced Energy Materials*, vol. 6, no. 3, pp. 1–19, 2016.
- [11] S. Pitchaiya, M. Natarajan, A. Santhanam, V. Asokan, A. Yuvapragasam, Venkatraman M. Ramakrishnan, S. E. Palanisamy, S. Sundaram, D. Velauthapillai, "A Review on the Classifications of Organic / Inorganic / Carbonaceous Hole Transporting Materials for Perovskite Solar Cell Application," *Arabian Journal of Chemistry*, 2018.
- [12] A. B. Coulibaly, S. O. Oyedele, N. R. Kre, and B. Aka, "Comparative Study of Lead-Free Perovskite Solar Cells Using Different Hole Transporter Materials," *Modeling and Numerical Simulation of Material Science*, vol. 09, no. 04, pp. 97–107, 2019.
- [13] K. Zhao, G. O. N. Ndjawa, L. K. Jagadamma, A. El Labban, H. Hu, Q. Wang, R. Li, M. Abdelsamie, Pierre M. Beaujuge, A. Amassian, "Highly efficient organic solar cells based on a robust room-temperature solution-processed copper iodide hole transporter," *Nano Energy*, vol. 16, pp. 458–469, 2015.
- [14] Y. Cao, Y. Saygili, A. Ummadisingu, J. Teuscher, J. Luo, N. Pellet, F. Giordano, S. M. Zakeeruddin, J. E. Moser, M. Freitag, A. Hagfeldt, and Michael Gratzel, "11% efficiency solid-state dye-sensitized solar cells with copper(II/I) hole transport materials," *Nature Communications*, vol. 8, pp. 1–8, 2017.
- [15] G. A. Sepalage, S. Meyer, A. Pascoe, A. D. Scully, F. Huang, U. Bach, Y. B. Cheng, and L. Spiccia "Copper(I) Iodide as Hole-Conductor in Planar Perovskite Solar Cells: Probing the Origin of J-V Hysteresis," *Advanced Functional Materials*, vol. 25, no. 35, pp. 5650–5661, 2015.

- [16] W. Y. Chen, L. Deng, S. Dai, X. Wang, C. Tian, X. Zhan, S. Xie, R. Huang and L. Zheng “Low-cost solution-processed copper iodide as an alternative to PEDOT:PSS hole transport layer for efficient and stable inverted planar heterojunction perovskite solar cells,” *Journal of Materials Chemistry A*, vol. 3, no. 38, pp. 19353–19359, 2015.
- [17] J. E. Jaffe, T. C. Kaspar, T. C. Droubay, T. Varga, M. E. Bowden, and G. J. Exarhos, “Electronic and defect structures of CuSCN,” *Journal of Physical Chemistry C*, vol. 114, no. 19, pp. 9111–9117, 2010.
- [18] A. C. Busacca V. Rocca, L. Curcio, A. Parisi, A. Cino, R. Pernice, A. Ando, G. Adamo, A. Tomasino, G. Palmisano, S. Stivala, M. Caruso, G. Cipriani, D. La Cascia, V. Di Dio, and G. Ricco Galluzzo, R. Miceli, “Parametrical study of multilayer structures for CIGS solar cells,” *2014 International Conference on Renewable Energy Research and Application (ICRERA)*, Milwaukee, pp. 964–968, October 2014.
- [19] J. H. Lee, B. H. Lee, J. Kang, M. Diware, K. Jeon, C. Jeong, S. Y. Lee, and K. H. Kim “Characteristics and electronic band alignment of a transparent P-CuI/N-SiZnSnO heterojunction diode with a high rectification ratio,” *Nanomaterials*, vol. 11, no. 5, 2021.
- [20] A. S. Subbiah, A. Halder, S. Ghosh, N. Mahuli, G. Hodes, and S. K. Sarkar, “Inorganic hole conducting layers for perovskite-based solar cells,” *Journal of Physical Chemistry Letters*, vol. 5, no. 10, pp. 1748–1753, 2014.
- [21] J. Wang, J. Li, and S. S. Li, “Native p-type transparent conductive CuI via intrinsic defects,” *Journal of Applied Physics*, vol. 110, no. 5, 2011.
- [22] J. Zhu, M. Gu, and R. Pandey, “Structural and electronic properties of CuI doped with Zn, Ga and Al,” *Journal of Physics and Chemistry of Solids*, vol. 74, no. 8, pp. 1122–1126, 2013.
- [23] K. M. S. Benbouza, D. Hocine, Y. Zid, A. Benbouza, “New nanotechnology structures CNTFET GaAs”, *8th International Conference on Renewable Energy Research and Applications (ICRERA)*, Romania, pp. 799–803, November 2019.
- [24] G. R. A. Kumara, S. Kaneko, M. Okuya, and K. Tennakone, “Fabrication of dye-sensitized solar cells using triethylamine hydrothiocyanate as a CuI crystal growth inhibitor,” *Langmuir*, vol. 18, no. 26, pp. 10493–10495, 2002.
- [25] K. Tennakone, G. R. R. A. Kumara, I. R. M. Kottegoda, V. P. S. Perera, G. M. L. P. Aponsu, and K. G. U. Wijayantha, “Deposition of thin conducting films of CuI on glass,” *Solar Energy Materials and Solar Cells*, vol. 55, no. 3, pp. 283–289, 1998.
- [26] V. P. S. Perera and K. Tennakone, “Recombination processes in dye-sensitized solid-state solar cells with CuI as the hole collector,” *Solar Energy Materials and Solar Cells*, vol. 79, no. 2, pp. 249–255, 2003.
- [27] N. S. Noorasid, F. Arith, A. N. Mustafa, M. A. Azam, S. Mahalingam, P. Chelvanathan and N. Amin, “Current Advancement of Flexible Dye Sensitized Solar Cell: A Review,” *Optik*, vol. 254, 168089, 2022.
- [28] C. A. N. Fernando and I. Kumarawadu, “Colloidal p-CuI-sensitized double-dye system,” *Semiconductor Science Technology*, 15 vol. 214, pp. 2–7, 2000.
- [29] S. Koyasu, N. Umezawa, A. Yamaguchi, and M. Miyauchi, “Optical properties of single crystalline copper iodide with native defects: Experimental and density functional theoretical investigation,” *Journal of Applied Physics*, vol. 125, no. 11, 2019.
- [30] C. Yang, M. Kneib, M. Lorenz, and M. Grundmann, “Room-Temperature synthesized copper iodide thin film as degenerate p-Type transparent conductor with a boosted figure of merit,” *Proceedings of the National Academy of Sciences of the United States of America*, vol. 113, no. 46, pp. 12929–12933, 2016.
- [31] D. Ahn, J. D. Song, S. S. Kang, J. Y. Lim, S. H. Yang, S. Ko, S. H. park, S. J. Park, D. S. Kim, H. J. Chang & J. Chang, “Intrinsically p-type cuprous iodide semiconductor for hybrid light-emitting diodes,” *Scientific Reports*, vol. 10, no. 1, pp. 1–8, 2020.
- [32] Y. Peng, N. Yaacobi-Gross, A. K. Perumal, H. A. Faber, G. Vourlias, P. A. Patsalas, D. D. C. Bradley, Z. He, and T. D. Anthopoulos “Efficient organic solar cells using copper(I) iodide (CuI) hole transport layers,” *Applied Physics Letters*, vol. 106, no. 24, pp. 1–4, 2015.
- [33] M. N. Amalina and M. Rusop, “Investigation on the I<sub>2</sub>:CuI thin films and its stability over time,” *Microelectronic Engineering*, vol. 108, pp. 106–111, 2013.
- [34] A. Nizamuddin, F. Arith, I.J. Rong, M. Zaimi, A.S. Rahimi, S. Saat, Investigation of Copper(I)Thiocyanate (CuSCN) as a Hole Transporting Layer for Perovskite Solar Cells Application, *Journal of Advanced Research in Fluid Mechanics and Thermal Sciences*, 78, pp. 153–159, 2021.
- [35] C. Moditswe, C. M. Muiva, P. Luhanga, and A. Juma, “Effect of annealing temperature on structural and optoelectronic properties of  $\gamma$ -CuI thin films prepared by the thermal evaporation method,” *Ceramics International*, vol. 43, no. 6, pp. 5121–5126, 2017.
- [36] M. Zi, J. Li, Z. Zhang, X. Wang, J. Han, X. Yang, Z. Qiu, H. Gong, Z. Ji, and B. Cao “Effect of deposition temperature on transparent conductive properties of  $\gamma$ -CuI film prepared by vacuum thermal evaporation,” *Physica Status Solidi (A) Applications and Materials Science*, vol. 212, no. 7, pp. 1466–1470, 2015.
- [37] Á. Balog, G. F. Samu, P. V. Kamat, and C. Janáky, “Optoelectronic Properties of CuI Photoelectrodes,” *Journal of Physical Chemistry Letters*, vol. 10, no. 2, pp. 259–264, 2019.
- [38] M. Cota-Leal, D. Cabrera-German, M. Sotelo-Lerma, M. Martínez-Gil, and J. A. García-Valenzuela, “Highly-

- transparent and conductive CuI films obtained by a redirected low-cost and electroless two-step route: Chemical solution deposition of CuS<sub>2</sub> and subsequent iodination,” *Materials Science in Semiconductor Processing*, vol. 95, no. 1, pp. 59–67, 2019.
- [39] A. R. Kumarasinghe, W. R. Flavell, A. G. Thomas, A. K. Mallick, D. Tsoutsou, C. Chatwin, S. Rayner, P. Kirkham, S. Warren, S. Patel, P. Christian, P. O’Brien, M. Grätzel, and R. Hengerer “Electronic properties of the interface between p-CuI and anatase-phase n-TiO<sub>2</sub> single crystal and nanoparticulate surfaces: A photoemission study,” *Journal of Chemical Physics*, vol. 127, no. 11, 2007.
- [40] X. Li, J. Yang, Q. Jiang, W. Chu, D. Zhang, Z. Zhou, and J. Xin, “Synergistic Effect to High-Performance Perovskite Solar Cells with Reduced Hysteresis and Improved Stability by the Introduction of Na-Treated TiO<sub>2</sub> and Spraying-Deposited CuI as Transport Layers,” *ACS Applied Materials and Interfaces*, vol. 9, no. 47, pp. 41354–41362, 2017.
- [41] W. Sun, S. Ye, H. Rao, Y. Li, Z. Liu, L. Xiao, Z. Chen, Z. Bian and C. Huang “Room-temperature and solution-processed copper iodide as the hole transport layer for inverted planar perovskite solar cells,” *Nanoscale*, vol. 8, no. 35, pp. 15954–15960, 2016.
- [42] S. Z. Haider, H. Anwar, Y. Jamil, and M. Shahid, “A comparative study of interface engineering with different hole transport materials for high-performance perovskite solar cells,” *Journal of Physics and Chemistry of Solids*, vol. 136, no. 7, p. 109147, 2020.
- [43] L. Zhang, X. Liu, J. Li, and S. McKechnie, “Interactions between molecules and perovskites in halide perovskite solar cells,” *Solar Energy Materials and Solar Cells*, vol. 175, no. 8, pp. 1–19, 2018.
- [44] N.S. Nooraid, F. Arith, A.N. Mustafa, M.A. Azam, S.H. Meriam Suhaimy, O.A. Al-ani, “Effect of Low Temperature Annealing on Anatase TiO<sub>2</sub> Layer as Photoanode for Dye-Sensitized Solar Cell,” *Przeegląd Elektrotechniczny*, vol. 97, no. 10, pp. 12–16, 2021.
- [45] T. Prakash, “Influence of temperature on physical properties of copper (I) iodide,” *Advanced Materials Letters*, vol. 2, no. 2, pp. 131–135, 2011.
- [46] D. K. Kaushik, M. Selvaraj, S. Ramu, and A. Subrahmanyam, “Thermal evaporated Copper Iodide (CuI) thin films: A note on the disorder evaluated through the temperature dependent electrical properties,” *Solar Energy Materials and Solar Cells*, vol. 165, no. 10, pp. 52–58, 2017.
- [47] R. Mulla and M. K. Rabinal, “Defect-Controlled Copper Iodide: A Promising and Ecofriendly Thermoelectric Material,” *Energy Technology*, vol. 6, no. 6, pp. 1178–1185, 2018.
- [48] M. M. Salah, K. M. Hassan, M. Abouelatta, and A. Shaker, “A comparative study of different ETMs in perovskite solar cell with inorganic copper iodide as HTM,” *Optik*, vol. 178, no. 10, pp. 958–963, 2019.
- [49] F. Arith, S.A.M. Anis, M.M. Said, C.M.I. Idris, “Low cost electro-deposition of cuprous oxide P-N homojunction solar cell,” *Advanced Materials Research*, 827 pp 38–43, 2014.
- [50] M. Huangfu, Y. Shen, G. Zhu, K. Xu, M. Cao, F. Gu, and L. Wang “Copper iodide as inorganic hole conductor for perovskite solar cells with different thickness of mesoporous layer and hole transport layer,” *Applied Surface Science*, vol. 357, pp. 2234–2240, 2015.
- [51] I. Massiot “Design and Fabrication of Nanostructures for Light-Trapping in Ultra-Thin Solar Cells,” Ph.D. Thesis, Université Paris Sud-Paris XI, Paris, France, 2013.
- [52] P. P. Murmu, V. Karthik, S. V. Chong, S. Rubanov, Z. Liu, T. Mori, J. Yi, and J. Kennedy “Effect of native defects on thermoelectric properties of copper iodide films,” *Emergent Materials*, vol. 4, no. 3, pp. 761–768, 2021.
- [53] N. S. Nooraid, F. Arith, A. Y. Firhat, A. N. Mustafa and A. S. Mohd Shah, SCAPS Numerical Analysis of Solid-State Dye-Sensitized Solar Cell Utilizing Copper (I) Iodide as Hole Transport Layer, *Engineering Journal*, vol. 26, no. 2, pp. 1-10, 2022.
- [54] O. V. Aliyasevum, S. A. Mat Junos, F. Arith, N. Izlan, M. Mohd Said, A. N. Mustafa, “Optimization of Copper(I) Thiocyanate as Hole Transport Material for Solar Cell by Scaps-1D Numerical Analysis”, *Przeegląd Elektrotechniczny*, vol. 98, no. 6, 2022.
- [55] A. Konno, T. Kitagawa, H. Kida, G. R. A. Kumara, and K. Tennakone, “The effect of particle size and conductivity of CuI layer on the performance of solid-state dye-sensitized photovoltaic cells,” *Current Applied Physics*, vol. 5, no. 2, pp. 149–151, 2005.
- [56] A. S. A. A. Elgharbawy, “Review on corrosion in solar panels,” *International Journal of Smart Grid-ijSmartGrid*, vol. 2, no. 4, pp. 218–220, 2018.
- [57] A. Bari, J. Jiang, W. Saad, and A. Jaekel, “Challenges in the smart grid applications: an overview,” *International Journal of Distributed Sensor Networks*, vol. 10, no. 2, p. 974682, 2014.